Zhang, Jian-Bo; Bowman, Patrick Oswald; Coad, Ryan J.; Heller, Urs M.; Leinweber, Derek Bruce; Williams, Anthony Gordon, CSSM Lattice Collaboration

Quark propagator in Landau and Laplacian gauges with overlap fermions Physical Review D, 2005; 71(1):014501

http://link.aps.org/doi/10.1103/PhysRevD.71.014501

Quark propagator in Landau and Laplacian gauges with overlap fermions

J. B. Zhang,[1] Patrick O. Bowman,[1,2] Ryan J. Coad,[1] Urs M. Heller,[3] Derek B. Leinweber,[1] and Anthony G. Williams[1]

(CSSM Lattice Collaboration)

[1]*Special Research Center for the Subatomic Structure of Matter (CSSM) and Department of Physics, University of Adelaide 5005, Australia*
[2]*Nuclear Theory Center, Indiana University, Bloomington, Indiana 47405, USA*
[3]*American Physical Society, One Research Road, Box 9000, Ridge, New York 11961-9000, USA*
(Received 1 November 2004; published 13 January 2005)

The properties of the momentum space quark propagator in Landau gauge and Gribov copy free Laplacian gauge are studied for the overlap quark action in quenched lattice QCD. Numerical calculations are done on two lattices with different lattice spacing a and the same physical volume. We have calculated the nonperturbative wave-function renormalization function $Z(q)$ and the nonperturbative mass function $M(p)$ for a variety of bare quark masses and perform a simple linear extrapolation to the chiral limit. We focus on the comparison of the behavior of $Z(q)$ and $M(p)$ in the chiral limit in the two gauge fixing schemes as well as the behavior on two lattices with different lattice spacing a. We find that the mass functions $M(p)$ are very similar for the two gauges while the wave-function renormalization function $Z(q)$ is more strongly infrared suppressed in the Laplacian gauge than in the Landau gauge on the finer lattice. For Laplacian gauge, it seems that the finite a error is large on the coarse lattice which has a lattice spacing a of about 0.124 fm.

DOI: 10.1103/PhysRevD.71.014501 PACS numbers: 12.38.Gc, 11.15.Ha, 12.38.Aw, 14.65.−q

I. INTRODUCTION

Quantum Chromodynamics (QCD) is widely accepted as the correct theory of the strong interaction and the quark propagator is one of its fundamental quantities. By studying the momentum-dependent quark mass function in the infrared region we can gain valuable insight into the mechanism of dynamical chiral symmetry breaking and the associated dynamical generation of mass. At high momenta, one can use the quark propagator to extract the running quark mass [1].

Lattice QCD provides a way to study the quark propagator nonperturbatively. There have been several lattice studies of the momentum space quark propagator [2–11] using different fermion actions. The usual gauge for these studies has been Landau gauge, because it is a (lattice) Lorentz covariant gauge that is easy to implement on the lattice, and the results from the lattice Landau gauge can be easily compared to studies that use different methods. Finite volume effects and discretization errors have been extensively explored in lattice Landau gauge [10,11]. Unfortunately, lattice Landau gauge suffers from the well-known problem of Gribov copies. Although the ambiguity originally noticed by Gribov [12] is not present on the lattice, since in practice one never samples from the same gauge orbit twice, the maximization procedure used for gauge fixing does not uniquely fix the gauge. In general, there are many local maxima for the algorithm to choose from, each one corresponding to a Gribov copy, and no local algorithm can choose the global maximum from among them. While various remedies have been proposed [13,14], they are either unsatisfactory or computationally very intensive. For a recent discussion of the Gribov problem in lattice gauge theory, see Ref. [15].

An alternative approach is to work with the so-called Laplacian gauge [16]. This gauge is ''Landau like'' in the sense that it has similar smoothness and Lorentz invariance properties [17], but it involves a nonlocal gauge fixing procedure that avoids lattice Gribov copies. The gluon propagator has already been studied in Laplacian gauge in Refs. [18,19] and the improved staggered quark propagator in Laplacian gauge in Ref. [6]. It has been shown [20] that Landau and Laplacian gauges become equivalent in the perturbative (high-momentum) regime and this has been confirmed by numerical studies [6,18,19].

In this paper we study the overlap quark propagator in the Laplacian gauge and compare the results with the Landau gauge to explore the effects of selecting a gauge condition free of Gribov copies. Unlike Asqtad fermions, the overlap formalism provides a fermion action which is free of doublers and preserves an exact form of chiral symmetry on the lattice. The latter feature makes overlap fermions the action of choice for studying dynamical chiral symmetry breaking near the chiral limit.

We also compare Laplacian gauge results on two lattices with the same physical volume and different lattice spacings a to explore the finite a error. In this work, the $\mathcal{O}(a^2)$ mean-field improved gauge action is used to generate the quenched gauge configurations.

II. GAUGE-FIXING

We consider the quark propagator in Landau and Laplacian gauges. Landau gauge fixing is performed by

enforcing the Lorentz gauge condition, $\sum_\mu \partial_\mu A_\mu(x) = 0$ on a configuration by configuration basis. For the tadpole improved plaquette plus rectangle (Lüscher-Weisz [21]) gauge action which we use in the current work, we use the $\mathcal{O}(a^2)$ improved gauge-fixing scheme, this is achieved by maximizing the functional [22],

$$\mathcal{F} = \frac{4}{3}\mathcal{F}_1 - \frac{1}{12u_0}\mathcal{F}_2, \tag{1}$$

where $\mathcal{F}_1$ and $\mathcal{F}_2$ are

$$\mathcal{F}_1 = \frac{1}{2}\sum_{x,\mu} \mathrm{Tr}\{U_\mu(x) + U_\mu^\dagger(x)\}$$

and

$$\mathcal{F}_2 = \frac{1}{2}\sum_{x,\mu} \mathrm{Tr}\{U_\mu(x)U_\mu(x+\mu) + U_\mu^\dagger(x+\mu)U_\mu^\dagger(x)\}$$

respectively, and u_0 is the usual plaquette measure of the mean link. In this case, a Fourier accelerated, steepest-descents algorithm [23] is used to find a local maximum. There are, in general, many local maxima and these are called lattice Gribov copies. This ambiguity in principle will remain a source of uncontrolled systematic error.

Laplacian gauge fixing is a nonlinear gauge fixing that respects rotational invariance, has been seen to be smooth, yet is free of Gribov ambiguity. It is also computationally cheaper then Landau gauge fixing. There is, however, more than one way of obtaining such a gauge fixing in SU(N) lattice gauge theory. There are three implementations of Laplacian gauge-fixing employed in the literature:

(1) ∂^2(I) gauge (QR decomposition), used by Alexandrou *et al.* [18].
(2) ∂^2(II) gauge, where the Laplacian gauge transformation is projected onto SU(3) by maximizing its trace [19].
(3) ∂^2(III) gauge (Polar decomposition), the original prescription described in Ref. [16] and tested in Ref. [17].

All three versions reduce to the same gauge in SU(2). For a more detailed discussion, see Ref. [19]. For SU(3) staggered quarks, the study in Ref. [6] indicate that ∂^2(I) and ∂^2(II) gauge give very similar results, and ∂^2(III) gauge is very noisy. In this work we will only use the ∂^2(II) gauge.

III. QUARK PROPAGATOR ON THE LATTICE

In a covariant gauge in the continuum, the renormalized Euclidean space quark propagator has the form

$$S(\zeta^2; p) = \frac{1}{i\not{p}A(\zeta^2; p^2) + B(\zeta^2; p^2)} = \frac{Z(\zeta^2; p^2)}{i\not{p} + M(p^2)}, \tag{2}$$

where ζ is the renormalization point. The renormalization point boundary conditions are chosen to be

$$Z(\zeta^2; \zeta^2) \equiv 1 \qquad M(\zeta^2) \equiv m(\zeta^2). \tag{3}$$

where $m(\zeta^2)$ is the renormalized quark mass at the renormalization point. The functions $A(\zeta^2; p^2)$ and $B(\zeta^2; p^2)$, or alternatively $Z(\zeta^2; p^2)$ and $M(p^2)$, contain all of the nonperturbative information of the quark propagator. Note that $M(p^2)$ is renormalization point independent, all of the renormalization-point dependence is carried by $Z(\zeta^2; p^2)$.

When all interactions for the quarks are turned off, i.e., when the gluon field vanishes (or the links are set to one), the quark propagator has its tree-level form

$$S^{(0)}(p) = \frac{1}{i\not{p} + m^0}, \tag{4}$$

where m^0 is the bare quark mass. When the interactions with the gluon field are turned on we have

$$S^{(0)}(p) \rightarrow S^{\mathrm{bare}}(a; p) = Z_2(\zeta^2; a)S(\zeta^2; p), \tag{5}$$

where a is the regularization parameter—in this case, the lattice spacing—and $Z_2(\zeta^2; a)$ is the quark wave-function renormalization constant chosen so as to ensure $Z(\zeta^2; p^2)|_{p^2=\zeta^2} = 1$. For simplicity of notation we suppress the a-dependence of the bare quantities.

On the lattice we expect the bare quark propagators, in momentum space, to have a similar form as in the continuum, except that the $O(4)$ invariance is replaced by a 4-dimensional hypercubic symmetry on an isotropic lattice. Hence, the inverse lattice bare quark propagator takes the general form

$$(S^{\mathrm{bare}})^{-1}(p) \equiv i[\sum_\mu C_\mu(p)\gamma_\mu] + B(p). \tag{6}$$

With the periodic boundary conditions in the spatial directions and antiperiodic in the time direction, the discrete lattice momenta will be

$$p_i = \frac{2\pi}{N_i a}\left(n_i - \frac{N_i}{2}\right), \quad \text{and} \quad p_t = \frac{2\pi}{N_t a}\left(N_t - \frac{1}{2} - \frac{N_t}{2}\right), \tag{7}$$

where $n_i = 1, .., N_i$ and $n_t = 1, .., N_t$, N_i and N_t are the lattice extent in spatial and temporal direction, respectively.

The overlap fermion formalism [24,25] realizes an exact chiral symmetry on the lattice and is automatically $\mathcal{O}(a)$ improved. The massive overlap operator can be written as [26]

$$D(\eta) = \frac{1}{2}[1 + \eta + (1 - \eta)\gamma_5\epsilon(H_w)], \tag{8}$$

where $H_w(x, y) = \gamma_5 D_w(x, y)$ is the Hermitian Wilson-Dirac operator, $\epsilon(H_w) = H_w/\sqrt{H_w^2}$ is the matrix sign function, and the dimensionless quark mass parameter η is

$$\eta \equiv \frac{m^0}{2m_w}, \tag{9}$$

where m^0 is the bare quark mass and m_w is the Wilson

quark mass which, in the free case, must be in the range $0 < m_w < 2$. The bare quark propagator in coordinate space is given by the equation

$$S^{\text{bare}}(m^0) \equiv \tilde{D}_c^{-1}(\eta), \tag{10}$$

where

$$\begin{aligned} \tilde{D}_c^{-1}(\eta) &\equiv \frac{1}{2m_w}\tilde{D}^{-1}(\eta) \quad \text{and} \\ \tilde{D}^{-1}(\eta) &\equiv \frac{1}{1-\eta}[D^{-1}(\eta) - 1] \end{aligned} \tag{11}$$

When all the interactions are turned off, the inverse bare lattice quark propagator becomes the tree-level version of Eq. (6)

$$(S^{(0)})^{-1}(p) \equiv i[\sum_{\mu} C_{\mu}^{(0)}(p)\gamma_{\mu}] + B^{(0)}(p). \tag{12}$$

We calculate $S^{(0)}(p)$ directly by setting the links to unity in the coordinate space, doing the matrix inversion and then taking its Fourier transform. It is then possible to identify the appropriate kinematic lattice momentum q directly from the definition

$$q_{\mu} \equiv C_{\mu}^{(0)}(p). \tag{13}$$

The form of $q_{\mu}(p_{\mu})$ is shown and its analytic form given in Ref. [9]. Having identified the appropriate kinematical lattice momentum q, we can now define the bare lattice propagator as

$$S^{\text{bare}}(p) \equiv \frac{Z(p)}{i\not{q} + M(p)}. \tag{14}$$

This ensures that the free lattice propagator is identical to the free continuum propagator. Because of asymptotic freedom the lattice propagator will also take the continuum form at large momenta. In the gauge sector, this type of analysis dramatically improves the gluon propagator [27–29].

The two Lorentz invariants can then obtained by

$$Z^{-1}(p) = \frac{1}{12iq^2}\text{Tr}\{\not{q}S^{-1}(p)\} \tag{15}$$

$$M(p) = \frac{Z(p)}{12}\text{Tr}\{S^{-1}(p)\}. \tag{16}$$

This means that $Z(p)$ is directly dependent on our choice of momentum, q, while $M(p)$ is not.

IV. NUMERICAL RESULTS

A. Simulation parameters

In this paper we work on two lattices with different lattice spacing, a, and very similar physical volumes. The gauge configurations are created using a tadpole improved plaquette plus rectangle (Lüscher-Weisz [21]) gauge action through the pseudo-heat-bath algorithm. For each lattice size, 50 configurations are used. Lattice parameters are summarized in Table I. The lattice spacing a is determined from the static quark potential with a string tension $\sqrt{\sigma} = 440$ MeV [30].

Landau gauge fixing to the gauge configuration was done using a Conjugate Gradient Fourier Acceleration [31] algorithm with an accuracy of $\theta \equiv \sum |\partial_{\mu} A_{\mu}(x)|^2 < 10^{-12}$. The improved gauge-fixing scheme was used to minimize gauge-fixing discretization errors [22]. For the Laplacian gauge fixing, we only use the ∂^2(II) gauge [19]. In this case we construct the gauge transformation by projecting $M(x)$ constructed from the three lowest lying eigenmodes, onto SU(3) by means of trace maximisation. Effectively, we maximise the trace of $G(x)M(x)^{\dagger}$ by iteration over Cabibbo-Marinari SU(2) subgroups.

Our numerical calculation begins with an evaluation of the inverse of $D(\eta)$ with the unfixed gauge configurations, where $D(\eta)$ is defined in Eq. (8). We approximate the matrix sign function $\epsilon(H_w)$ by the 14th order Zolotarev approximation [32]. We then calculate Eq. (10) for each configuration and rotate it to Landau or Laplacian gauge by using the corresponding gauge transformation matrices $\{G_i(x)\}$. Afterward we take the ensemble average to obtain $S^{\text{bare}}(x, y)$. The discrete Fourier transformation is then applied to $S^{\text{bare}}(x, y)$ and the momentum-space bare quark propagator, $S^{\text{bare}}(p)$ is obtained finally.

We use the mean-field improved Wilson action in the overlap fermion kernel. The value $\kappa = 0.19163$ is used in the Wilson action, which provides $m_w a = 1.391$ for the regulator mass in the interacting case [9]. We calculate the overlap quark propagator for ten quark masses on each ensemble by using a shifted Conjugate Gradient solver. For the two lattices considered here, the quark mass parameter η was adjusted to make the tree-level bare quark mass in physical units, the same on the two lattices. For example, we choose $\mu = 0.018$, 0.021, 0.024, 0.030, 0.036, 0.045, 0.060, 0.075, 0.090, and 0.105 on ensemble 1, i.e., the $16^3 \times 32$ lattice with $a = 0.093$ fm. This corresponds to bare masses in physical units of $m^0 = 2\mu m_w = 106$, 124, 142, 177, 212, 266, 354, 442, 531, and 620 MeV, respectively.

The results of lattice 2 ($12^3 \times 24$) in Landau gauge were presented in detail in Ref. [9], and the results of lattice 1($16^3 \times 32$) in Landau gauge were also reported in Ref. [11]. Here we will focus on the comparison of the results of two lattice gauge-fixing schemes, i.e., the Landau gauge and the Gribov copy free Laplacian gauge, to probe the behavior of the overlap fermion propagator with different gauge fixings, and the effect of Gribov copies. Before we make the comparison, we first briefly present some data in Laplacian gauge on the $16^3 \times 32$ lattice, our fine lattice. All data has been cylinder cut [27]. Statistical uncertainties are estimated via a second-order, single-elimination jackknife.

TABLE I. Lattice parameters.

Action	Volume	N_{Therm}	N_{Samp}	β	a (fm)	u_0	Physical Volume (fm^4)
Improved	$16^3 \times 32$	5000	500	4.80	0.093	0.89 650	$1.5^3 \times 3.00$
Improved	$12^3 \times 24$	5000	500	4.60	0.124	0.88 888	$1.5^3 \times 3.00$

B. Laplacian gauge

In Fig. 1 we show the results for all ten masses for both the mass and wave-function renormalization functions, $M(p)$ and $Z^{(\mathrm{R})}(q) \equiv Z(\zeta; q)$ respectively. As was shown in Ref. [11], the continuum limit is more rapidly approached when the mass function is plotted against the discrete lattice momentum p, while the wave-function renormalization function $Z^{(\mathrm{R})}(q)$ is plotted against the kinematic momentum q. The renormalization point in Fig. 1 for $Z^{(\mathrm{R})}(q)$ has been chosen to be $\zeta = 5.31$ GeV in the q-scale.

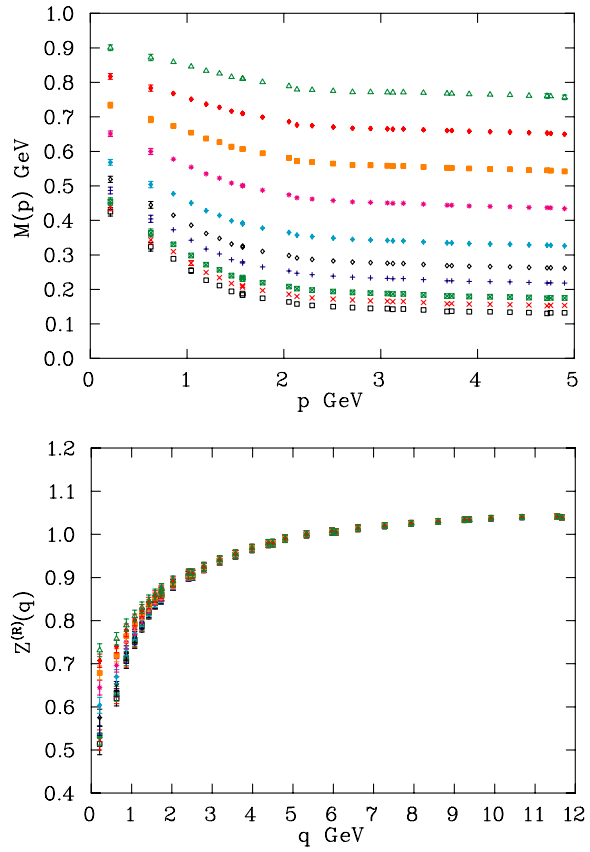

FIG. 1 (color online). The functions $M(p)$ and $Z^{(\mathrm{R})}(q) \equiv Z(\zeta^2; q)$ renormalized at $\zeta = 5.31$ GeV (in the q scale) for all ten quark masses in Laplacian gauge on the $16^3 \times 32$ lattice. The mass function $M(p)$ is plotted versus the discrete momentum p defined in Eq. (7), $p = \sqrt{\sum p_\mu^2}$, over the interval $[0, 5]$ GeV, and $Z^{(\mathrm{R})}(q)$ is plotted against the kinematic momentum q defined in Eq. (13), $q = \sqrt{\sum q_\mu^2}$, over the interval $[0, 12]$ GeV. The data correspond to bare quark masses (from bottom to top) $\mu =$ 0.018, 0.021, 0.024, 0.030, 0.036, 0.045, 0.060, 0.075, 0.090, and 0.105, which in physical units correspond to $m^0 = 2\eta m_w \simeq$ 106, 124, 142, 177, 212, 266, 354, 442, 531, and 620 MeV, respectively.

In the plots of $M(p)$, the data is ordered as one would expect by the values for bare quark mass m^0, i.e., the larger the bare quark mass m^0, the higher the $M(p)$ curve. For large momenta, the function $Z^{(\mathrm{R})}(q)$ demonstrates little mass dependence. Deviation of $Z^{(\mathrm{R})}(q)$ from its asymptotic value of one is a sign of dynamical symmetry breaking, so we expect the infrared suppression to vanish in the limit of an infinitely heavy quark. In the figure for $Z^{(\mathrm{R})}(q)$, the smaller the bare mass, the more pronounced is the dip at low momenta. Similarly, at small bare masses $M(q)$ falls off more rapidly with increasing momenta, which is understood from the fact that a larger proportion of the infrared mass is due to dynamical chiral symmetry breaking at small bare quark masses. These results are much the same as in Ref. [11], which display the data on the same lattices in Landau gauge. This qualitative behavior is also consistent with what is seen in Dyson-Schwinger based QCD models [33,34].

In Fig. 2 we plot the data after a linear chiral extrapolation for both functions $M(p)$ and $Z^{(\mathrm{R})}(q) \equiv Z(\zeta; q)$ in Laplacian gauge. The mass function $M(p)$ is shown against p and while the wave function renormalization function $Z^{(\mathrm{R})}(q)$ is shown against q with the renormalization-point chosen as at 5.31 GeV in the q scale. We see that both $M(p)$ and $Z^{(\mathrm{R})}(q)$ deviate strongly from the tree-level behavior, which are $M(p) = m^0$ and $Z^{(\mathrm{R})}(q) = 1$. In particular, as in earlier studies of the Landau gauge quark propagator[4–6,9,11], we find a clear signal of dynamical mass generation and a significant infrared suppression of the $Z(\zeta; q)$ function.

C. Gauge fixing comparison

Next we present the results in the two gauge fixing schemes for comparison. All data have been cylinder cut [27]. First we give the results on the $16^3 \times 32$ lattice.

Figure 3 reports results for the mass and renormalization functions at our lightest bare quark mass of $m^0 =$ 106 MeV. These results may be compared with the Asqtad results of Ref. [6], where Fig. 9 compares results of various gauge fixing schemes for the renormalization function. There, Landau gauge results are seen to lie significantly higher than the Laplacian gauge results

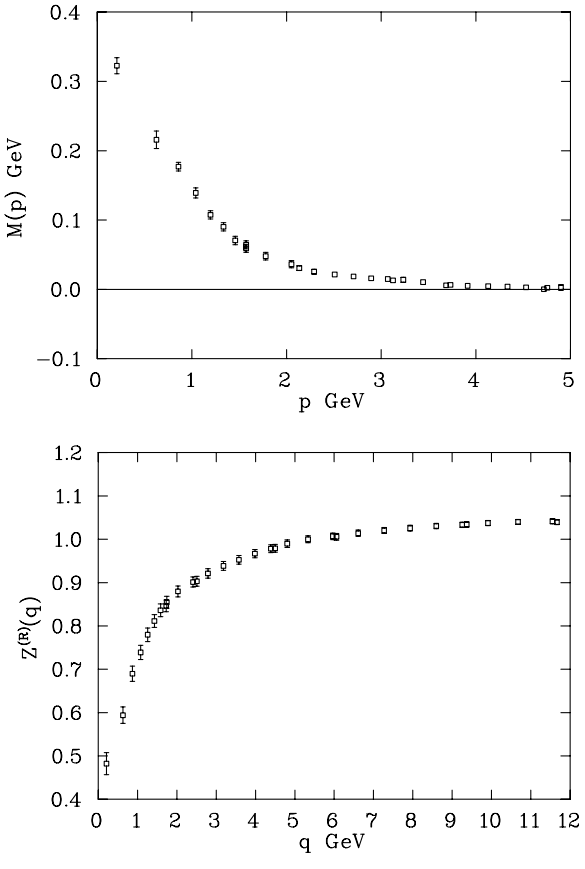

FIG. 2. The plot of the functions $M(p)$ and $Z^{(R)}(q) \equiv Z(\zeta; q)$ after a linear extrapolation to the chiral limit. The mass functions $M(p)$ is plotted against the discrete momentum p in the upper part of the figure and $Z^{(R)}(q)$ with the renormalization point $\zeta = 5.31$ GeV (in the q-scale) is plotted against the kinematic momentum q in the lower part of the figure.

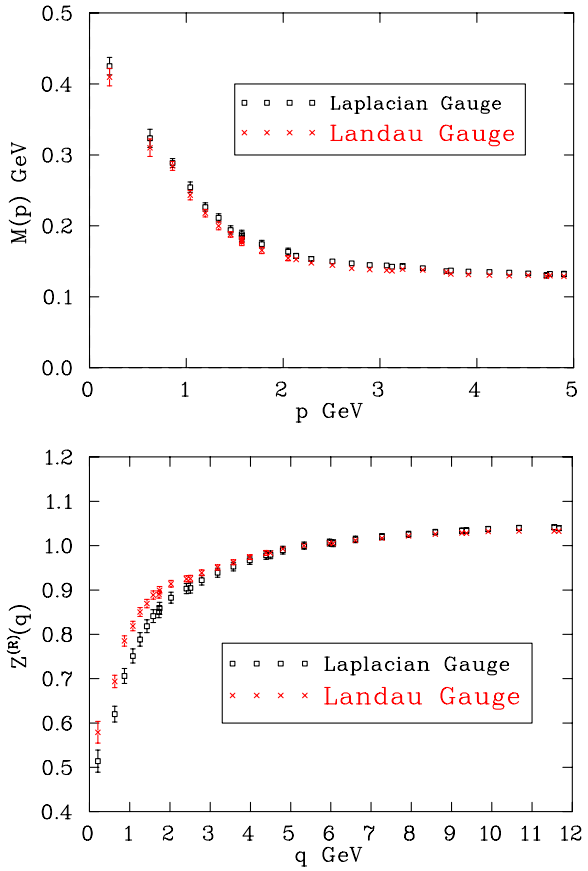

FIG. 3 (color online). The comparison of two gauge-fixing results at finite bare quark mass ($m^0 = 106$ MeV) on the fine $16^3 \times 32$ lattice with $a = 0.093$ fm. $Z^{(R)}(q)$ is renormalized to one at the renormalization point $\zeta = 5.31$ GeV (in the q-scale). For the mass function $M(p)$, Landau gauge and Laplacian gauge are very similar, while the wave function renormalization functions $Z^{(R)}(q)$ differ in the infrared region.

in the infrared. However, with overlap fermions, Fig. 3 indicates the Landau gauge results lie much closer to the Laplacian gauge results. Given the improved chiral properties of the overlap operator, the present results should provide a better indication of the continuum limit behavior. In either case, the same qualitative behavior of Landau Gauge sitting above Laplacian gauge in the infrared is observed.

The mass function of Fig. 3 reveals an approximate invariance on the selection of Landau or Laplacian gauges. Figures 12 and 13 of Ref. [6] indicate that the mass function of Asqtad fermions is also insensitive to the choice of Landau gauge or the Gribov-copy free Laplacian gauge.

We now proceed to compare the data in the chiral limit. Figure 4 shows the comparison of the mass function, $M(p)$, and the wave function renormalization function, $Z^{(R)}(q)$, in Landau gauge and Laplacian gauge. We see that they give similar performance in terms of rotational symmetry and statistical noise. Looking more closely, we can see that Landau gauge gives a slightly cleaner signal at this lattice spacing. We also note that at very large momenta, the two gauge fixing schemes give similar results as expected. Although Laplacian gauge is a nonlocal gauge fixing scheme and difficult to understand perturbatively, it is equivalent to Landau gauge in the asymptotic region [20]. In the infrared region, the mass function, $M(p)$, in the two gauges are very similar. For the mass functions there is a hint that the data in Laplacian gauge are a little higher than for the Landau gauge, although they agree within statistical errors. With greater statistics we may resolve a small difference. For the renormalization function $Z^{(R)}(q)$, there are systematic differences in the infrared region. The $Z^{(R)}(q)$ is more strongly infrared suppressed in the Laplacian gauge than in the Landau gauge. That is consistent with what was seen in the case of the Asqtad quark action [6] when comparing these two gauges.

Now we give the results from the coarse lattice. Figure 5 shows the comparison of the mass function $M(p)$ and the wave function renormalization function $Z^{(R)}(q)$ in the chi-

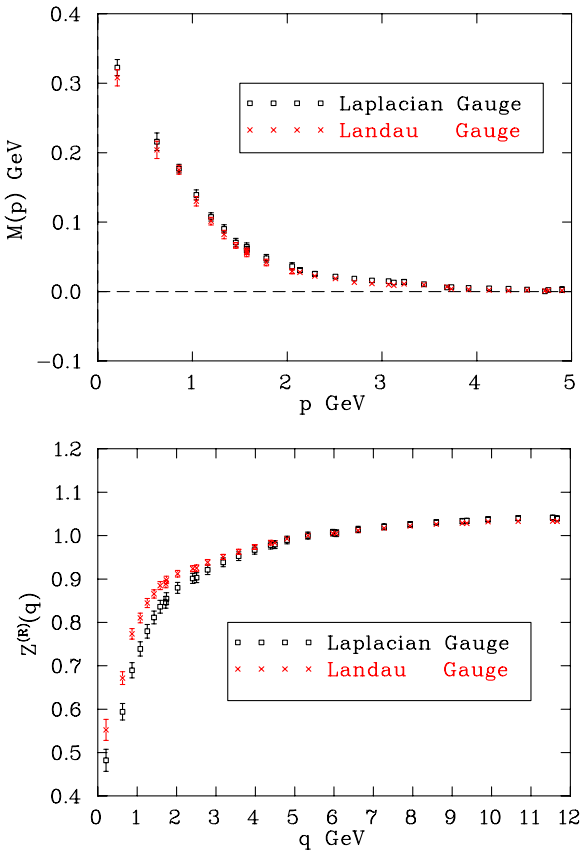

FIG. 4 (color online). The comparison of two gauge-fixing results after a linear extrapolation to the chiral limit on the fine lattice, i.e., $16^3 \times 32$ at $a = 0.093$ fm. $Z^{(R)}(q)$ is renormalized to one at the renormalization point $\zeta = 5.31$ GeV (in the q-scale). For the mass function $M(p)$, Landau gauge and Laplacian gauge are very similar, while the wave function renormalization functions $Z^{(R)}(q)$ are similar in the large momentum region but differ in the infrared region.

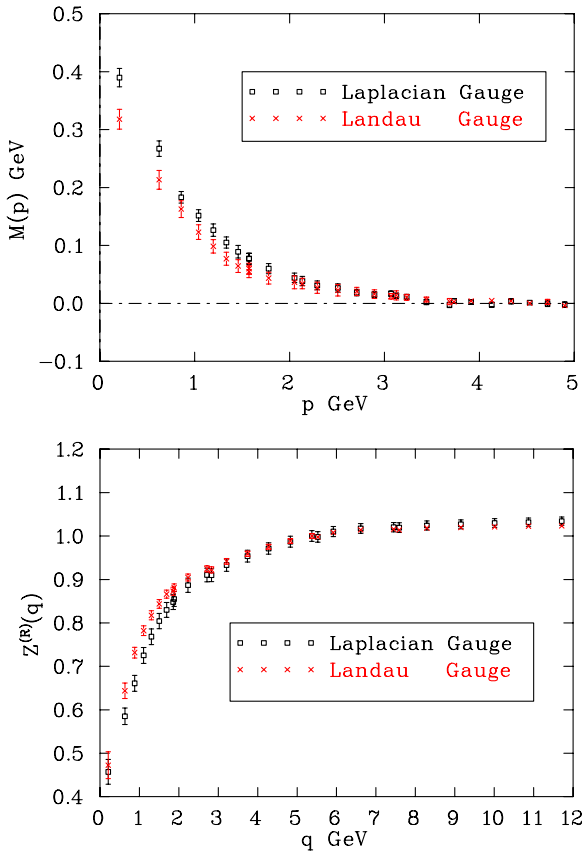

FIG. 5 (color online). The comparison of two gauge-fixing results in the chiral limit on the coarse lattice, i.e., $12^3 \times 24$ with $a = 0.124$ fm. The small gauge dependence of the infrared behavior of the Z-function is similar to that on the fine lattice in Fig. 4. The infrared mass functions, $M(p)$, appear different on this coarse lattice whereas they were similar on the fine lattice. This suggests larger $\mathcal{O}(a^2)$ errors in Laplacian gauge.

ral limit in Landau gauge and Laplacian gauge on the $12^3 \times 24$ lattice with $a = 0.124$ fm. As in the case of the $16^3 \times 32$ lattice, at very large momenta, the two gauge fixing schemes give similar results. For the renormalization function $Z^{(R)}(q)$, the situation is very similar to the case of the $16^3 \times 32$ lattice, i.e., at very large momenta, the two gauge fixing schemes give similar results, while in the infrared region, $Z^{(R)}(q)$ is more strongly suppressed in Laplacian gauge than in Landau gauge. For the mass function, $M(p)$, the situation is different to that seen on the fine lattice. In the infrared region, the data in Laplacian gauge sit higher than in Landau gauge. While this is consistent with the infrared behavior of the renormalization function, $Z^{(R)}(q)$, which is more suppressed in Laplacian gauge than in Landau gauge, there is no similar signal for our fine lattice $16^3 \times 32$. In that case (see Fig. 5), the data in Laplacian gauge agree with that in Landau gauge within error bars, although there is a hint that the data in Laplacian gauge are a little higher than in Landau gauge in the infrared region. This infrared behavior of the mass function in Laplacian gauge is likely caused by the finite lattice spacing errors, i.e., on fine enough lattices we expect Landau and Laplacian gauge results for $M(p)$ to be very similar.

Finally, we present the data for the two lattices in Laplacian gauge to further explore possible finite a errors. Figure 6 shows the comparison of the mass function, $M(p)$, and the wave function renormalization function $Z^{(R)}(q)$ in the chiral limit in Laplacian gauge on the $12^3 \times 24$ and the $16^3 \times 32$ lattices. For the renormalization function, $Z^{(R)}(q)$, results from the two lattices have small differences, but agree with each other within errors. For the mass function, $M(p)$, the results agree well at large momenta, but there is a substantial difference in the infrared region. A similar comparison was made between these two lattices in Landau gauge [11]. In that case, both the renormalization function, $Z^{(R)}(q)$, and the mass function, $M(p)$, agree well on the two lattices. This indicates that in Landau gauge, the finite a errors are small even for our coarse

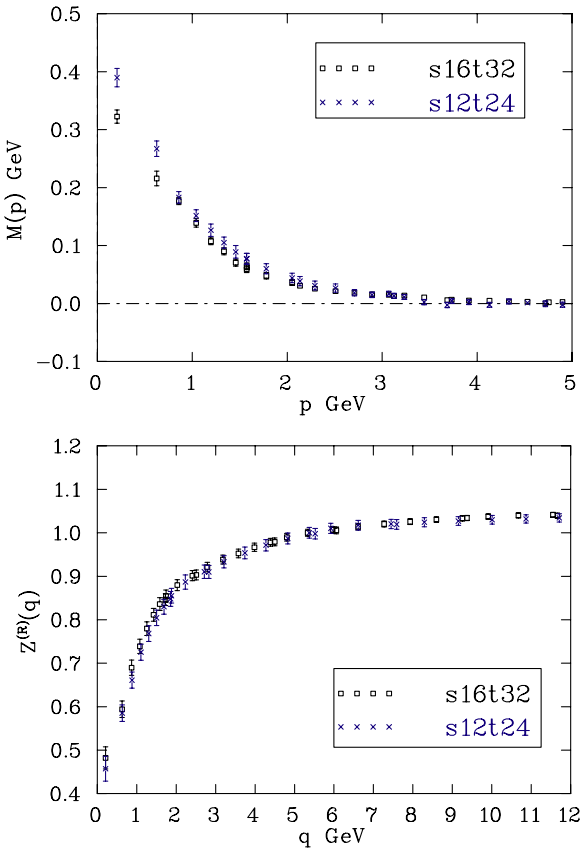

FIG. 6 (color online). The comparison of Laplacian gauge results in the chiral limit on two lattices, i.e., $12^3 \times 24$ with $a = 0.124$ fm and $16^3 \times 32$ with $a = 0.093$ fm. The renormalization point for $Z^{(R)}(q) \equiv Z(\zeta; q)$ is chosen to be $\zeta = 5.31$ GeV (in the q-scale). For the mass functions $M(p)$, the value on $12^3 \times 24$ lattice is higher than that on the $16^3 \times 32$ lattice in the infrared region. while the wave function renormalization function $Z^{(R)}(q)$ on two lattices agree within error bars. This suggests that the finite a errors are not small on the coarse lattice in Laplacian gauge.

lattice with lattice spacing $a = 0.124$ fm. But in Laplacian gauge, the finite a errors are not negligible for our coarse lattice $12^3 \times 24$. A likely explanation for this is the fact that our implementation of the Laplacian gauge is not $\mathcal{O}(a^2)$ improved.

V. SUMMARY AND OUTLOOK

The momentum-space quark propagator has been studied in Landau gauge as well as the Gribov copy free Laplacian gauge on two lattices with the same physical volume but with different lattice spacings a. We calculated the nonperturbative momentum-dependent wave-function renormalization, $Z(q)$, and the nonperturbative mass function, $M(p)$, for a variety of bare quark masses. We also performed a simple linear extrapolation to the chiral limit.

At very large momenta the two gauge-fixing schemes give similar results as expected. Laplacian gauge is equivalent to the Landau gauge in the asymptotic region. In the infrared region, the mass function, $M(p)$, in the two gauges are very similar on the fine lattice, but differ on the coarse lattice. The present Laplacian gauge fixing is not $\mathcal{O}(a^2)$ improved. For our fine lattice in the infrared region, the mass function, $M(p)$, agrees within statistical errors in the two gauge fixings. However, there is a hint that the data in Laplacian gauge may be a little higher than in Landau gauge, which would be consistent with the behavior of the renormalization function, $Z^{(R)}(q)$. For the renormalization function, $Z^{(R)}(q)$, there are systematic differences in the infrared region. The renormalization function is more strongly infrared suppressed in the Laplacian gauge than in the Landau gauge.

ACKNOWLEDGMENTS

We thank the Australian National Computing Facility for Lattice Gauge Theory and both the Australian Partnership for Advanced Computing (APAC) and the South Australian Partnership for Advanced Computing (SAPAC) for generous grants of supercomputer time which have enabled this project. This work is supported by the Australian Research Council.

[1] P. O. Bowman, U. M. Heller, D. B. Leinweber, A. G. Williams, and J. B. Zhang, Nucl. Phys. B, Proc. Suppl. **128**, 23 (2004).
[2] C. W. Bernard, D. Murphy, A. Soni, and K. Yee, Nucl. Phys. B, Proc. Suppl. **17**, 593 (1990).
[3] C. W. Bernard, A. Soni, and K. Yee, Nucl. Phys. B, Proc. Suppl. **20**, 410 (1991).
[4] J. I. Skullerud and A. G. Williams, Phys. Rev. D **63**, 054508 (2001); Nucl. Phys. B, Proc. Suppl. **83**, 209 (2000).
[5] J. Skullerud, D. B. Leinweber, and A. G. Williams, Phys. Rev. D **64**, 074508 (2001).
[6] P. O. Bowman, U. M. Heller, and A. G. Williams, Phys. Rev. D **66**, 014505 (2002).
[7] P. O. Bowman, U. M. Heller, D. B. Leinweber, and A. G. Williams, Nucl. Phys. B, Proc. Suppl. **119**, 323 (2003).
[8] T. Blum *et al.*, Phys. Rev. D **66**, 014504 (2002).
[9] F. D. R. Bonnet, P. O. Bowman, D. B. Leinweber, A. G. Williams, and J. B. Zhang, Phys. Rev. D **65**, 114503 (2002).

[10] J. B. Zhang, F. D. R. Bonnet, P. O. Bowman, D. B. Leinweber, and A. G. Williams, Nucl. Phys. B, Proc. Suppl. **129**, 495 (2004).
[11] J. B. Zhang, P. O. Bowman, D. B. Leinweber, A. G. Williams, and F. D. R. Bonnet, Phys. Rev. D **70**, 034505 (2004).
[12] V. N. Gribov, Nucl. Phys. **B139**, 1 (1978).
[13] J. E. Hetrick and Ph. de Forcrand, Nucl. Phys. B, Proc. Suppl. **63**, 838 (1998).
[14] J. F. Markham and T. D. Kieu, Nucl. Phys. B, Proc. Suppl. **73**, 868 (1999); O. Oliveira and P. J. Silva, Nucl. Phys. B, Proc. Suppl. **106**, 1088 (2002).
[15] A. G. Williams, Prog. Theor. Phys. Suppl. **151**, 154 (2003).
[16] J. C. Vink and U-J. Wiese, Phys. Lett. B **289**, 122 (1992).
[17] J. C. Vink, Phys. Rev. D **51**, 1292 (1995).
[18] C. Alexandrou, Ph. de Forcrand, and E. Follana, Phys. Rev. D **63**, 094504 (2001); **65**, 114508 (2002); **65**, 117502 (2002).
[19] P. O. Bowman, U. M. Heller, D. B. Leinweber, and A. G. Williams, Phys. Rev. D **66**, 074505 (2002).
[20] P. van Baal, Nucl. Phys. B, Proc. Suppl. **42**, 843 (1995).
[21] M. Lüscher and P. Weisz, Commun. Math. Phys. **97**, 59 (1985).
[22] F. D. R. Bonnet, P. O. Bowman, D. B. Leinweber, A. G. Williams, and D. G. Richards, Aust. J. Phys. **52**, 939 (1999).
[23] C. T. H. Davies *et al.*, Phys. Rev. D **37**, 1581 (1998).
[24] R. Narayanan and H. Neuberger Nucl. Phys. **B443**, 305 (1995).
[25] H. Neuberger, Phys. Lett. B **427**, 353 (1998).
[26] R. G. Edwards, U. M. Heller, and R. Narayanan, Phys. Rev. D **59**, 094510 (1999).
[27] D. B. Leinweber, J. I. Skullerud, A. G. Williams, and C. Parrinello, Phys. Rev. D **58**, 031501(R) (1998); **60**, 094507 (1999); **61**, 079901(E) (1999);
[28] F. D. R. Bonnet, P. O. Bowman, D. B. Leinweber, and A. G. Williams, Phys. Rev. D **62**, 051501(R) (2000).
[29] F. D. R. Bonnet, P. O. Bowman, D. B. Leinweber, A. G. Williams, and J. M. Zanotti, Phys. Rev. D **64**, 034501 (2001).
[30] F. D. R. Bonnet, D. B. Leinweber, A. G. Williams, and J. M. Zanotti, hep-lat/9912044.
[31] A. Cucchieri and T. Mendes, Phys. Rev. D **57**, R3822 (1998).
[32] J. van den Eshof *et al.*, Comput. Phys. Commun. **146**, 203 (2002); Nucl. Phys. B, Proc. Suppl. **106**, 1070 (2002).
[33] C. D. Roberts and A. G. Williams, Prog. Part. Nucl. Phys. **33**, 477 (1994).
[34] R. Alkofer and L. von Smekal, Phys. Rep. **353**, 281 (2001).